Proceedings of the International Convention of Society of Wood Science and Technology and United Nations Economic Commission for Europe – Timber Committee
October 11-14, 2010, Geneva, Switzerland

From Laboratory Corrosion Tests to a Corrosion Lifetime for Wood Fasteners: Progress and Challenges

Samuel L. Zelinka
US Forest Service Forest Products Laboratory
Madison WI, USA

Dominique Derome
Empa- Swiss Federal Laboratories for Materials Science and Technology
Dübendorf, Switzerland

Samuel V. Glass
US Forest Service Forest Products Laboratory
Madison WI, USA

Abstract

Determining a "corrosion-lifetime" for fasteners embedded in wood treated with recently adopted preservative systems depends upon successfully relating results of laboratory tests to in-service conditions. In contrast to laboratory tests where metal is embedded in wood at constant temperature and moisture content, the in-service temperature and moisture content of wood exhibit large fluctuations which affect the corrosion rate. The paper presents an approach for determining the corrosion lifetime of fasteners in which the calculated wood moisture content at the wood-fastener interface is used to predict the corrosion rate as a function of time through coupling two models. First, the moisture content across the wood component is calculated using a finite element code solving the coupled heat and mass transport equations with climatic data used as boundary conditions. Secondly, at the wood-fastener interface, the instantaneous corrosion rates are computed using an empirical corrosion model and integrated with time. Preliminary results for a simplified geometry are presented in this paper.

Keywords: Corrosion, hygrothermal modeling, preservative treated wood

Introduction

One aspect of the durability of treated wood structures is the lifetime of metallic fasteners. Their corrosion rate depends on the moisture and temperature conditions on the metallic surface, which vary considerably in outdoor wood construction such as terrace decks and balconies. In this paper, we present a computer simulation method to model the coupled phenomena of corrosion of metallic fasteners and heat and mass transport in wood.

Our corrosion model draws upon recent experimental work that followed a January 2004 wood preservation regulation change in the United States by which chromated copper arsenate (CCA) was replaced by alternatives such as alkaline copper quaternary (ACQ) and copper Azole (CuAz) for residential applications (Lebow 2004). Evidence suggested that the alternative wood preservatives might be more corrosive to metal fasteners embedded in the wood than CCA (Burkholder 2004; anon. 2008). From a practical perspective, it was necessary to select the correct type of corrosion resistant fasteners. This practical need motivated fundamental research with the ultimate goal of predicting the corrosion lifetime for metallic fasteners in treated wood. As a result, many tests were conducted to measure corrosion rates in wood treated with CCA alternatives.

The corrosiveness of CuAz and ACQ has been evaluated by several different test methods. Most of the previous research has used the American Wood Protection Association AWPA E-12 standard, which places metal coupons between blocks of wood and subjects them to a high temperature (49°C) environment at 90% relative humidity (RH) for at least 240 hours (Freeman & McIntyre 2008; Kear et al. 2009). Other procedures using different environmental conditions were developed. Kear et al. (2009) exposed fasteners embedded in treated wood to 21°C at 3 different relative humidities ranging from 75% to 98% RH for 1 year. Zelinka and Rammer (2009) embedded fasteners in blocks of treated wood exposing them to 27°C and 100% RH for one year. In a novel test procedure, electrochemical tests in a water-extract of treated wood were found to have the same corrosion rates as those measured at the 27°C 100% RH condition (Zelinka et al. 2008). These tests show that ACQ and CuAz are more corrosive than CCA. However, the different corrosion rates measured in these tests are quite variable. For example the corrosion rates range between 2-113 $\mu m\ yr^{-1}$ for hot-dip galvanized steel in ACQ treated wood. The difference in corrosion rates between test methods makes it difficult to use the data for corrosion design or durability prediction. The most likely cause for the range in corrosion rate is the differences in wood moisture content between the test methods.

It is widely known that the corrosion rate of metals in contact with wood depends strongly on the wood moisture content (MC). Below 15%-18% MC, embedded metals do not corrode (Baker 1987; Short & Dennis 1997). Above this threshold, the corrosion rate increases with increasing moisture content before eventually reaching a plateau (Kear et al. 2009; Short & Dennis 1997). Therefore, it is necessary to know the moisture contents of exposed wood structures when predicting a corrosion lifetime. Recent reviews of studies that examined the in-service moisture content of wood decks have shown that wood used in exterior applications experiences large variations in moisture content (from 8% to 80%) depending on the environmental conditions (Lebow & Lebow 2007; Glass & TenWolde 2007). These changes in the wood moisture content affect the corrosion rate at the wood-fastener interface; therefore a steady-state approximation of the corrosion rate is not able to capture these changes and predict a corrosion lifetime.

For predicting the corrosion lifetime of fasteners in treated wood, we propose to use hygrothermal modeling to calculate the conditions at the wood-fastener interface, i.e. moisture content and temperature, as a function of time. Several such models have been developed in the last 20 years. We use here an existing heat and moisture transport model (Janssen et al. 2007) to calculate conditions at the wood-fastener interface using a complete set of climatic data as boundary conditions which includes air temperature and relative humidity, solar radiation, cloud cover, rain precipitation and wind conditions. The coupling of the models is implemented by inputting the moisture content at the wood-fastener interface into a corrosion rate model that is dependent on MC. This paper presents preliminary work combining the corrosion and hygrothermal models, implemented on a simplified geometry. Future work will include validation with field corrosion studies and is described at the end of this paper,.

Model Development

In this section, we first present the geometry of the specific construction used in the model, followed by the corrosion model and the hygrothermal model. We then present details of the material properties before discussing how the models were coupled.

Geometry of the Physical Problem

We examine here the corrosion of the fasteners used to connect the decking to the joists (i.e. deck screws). We present first standard deck construction practice and then describe the simplified geometry used in the model.

The American Forest and Paper Association recently published a *Prescriptive Residential Wood Deck Construction Guide* based on the *2009 International Residential Code* (IRC) which gives the minimum construction requirements for single level residential wood decks. The guide gives two options for fastening decking to the joists: “8d” threaded nails (64 mm long, ~3 mm in diameter) or “#8” screws (4.2 mm major diameter). The nails or screws must be made of hot-dip galvanized steel, stainless steel, silicon bronze, or copper and two fasteners must be used at each joist. The guide states that decking material should be made of dimension lumber 38 mm thick (nominal 2 inch thickness) and that the deck boards should be spaced approximately 3.2 mm apart, although the width of the deck board is not specified. Similarly, the joists must also be made of dimension lumber 38 mm thick and at least 190 mm in width. The guide allows a variety of species to be used, although the most common decking material in the US is southern pine (*Pinus spp.*). The guide specifies that wood should be treated according to the appropriate

American Wood Protection Association standards (anon 2007). It is important to note that while these specifications represent a deck in compliance with the IRC, many decks are built by the homeowner after the original house is constructed and the materials and construction practices of decks are quite variable (West 2006).

In this modeling, several simplifications are made to the configuration. The modeled geometry as well as the mesh are shown in Figure 1**.** The first simplification is that in the model, the fastener is embedded in a single wooden beam, which can be thought of as a joist with the deck board removed. The second simplification is that the problem can be treated two-dimensionally, which is equivalent to assuming that the fastener is in the middle of an infinitely long beam. Thirdly, the fastener geometry is modeled as a smooth cylinder, instead of an annularly or helically threaded fastener. Symmetry considerations were used so that only half of the width needed to be modeled. The two dimensional mesh is 20 by 90 mm and consisted of 1965 elements and 2064 nodes. The fastener width was taken as 3.2 mm based on the width of a smooth 8d fastener. Heat and moisture transport through the fastener was not modeled; instead, the fastener was represented in the model by a "no-flow" boundary condition.

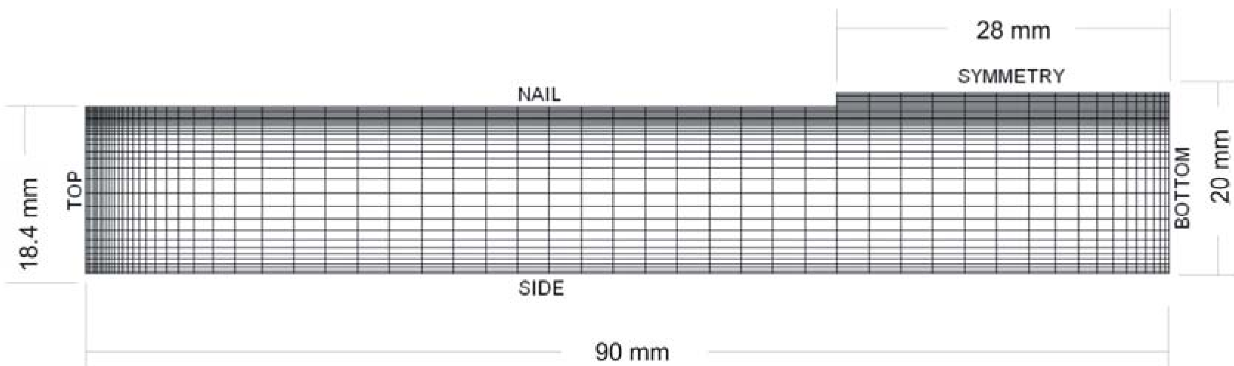

Figure 1: Mesh used for the hygrothermal model. Boundary conditions are explained in the Heat and Mass Transport Modeling section. The geometry describes one half of a "2 by 4" (38 mm by 90 mm) beam with an 8d nail, which is not included in the mesh.

Corrosion Modeling

Short and Dennis used electrochemical techniques to measure the corrosion rate of zinc as a function of moisture content (Short & Dennis 1997). They placed a small strip of CCA treated wood between the stainless steel counter electrode and the zinc working electrode. Two more pieces of wood were placed on the outside of the working and counter electrodes to create a "sandwich". The wood moisture content was adjusted by placing the assembly in various conditioning chambers and the corrosion rate was measured using polarization resistance[1]. Short and Dennis found a sigmoidal dependence of the corrosion rate on moisture content: below 15% moisture content, there was no corrosion and above 27% moisture content, the corrosion rate was constant at its maximum value. Their data for the corrosion rate (R) as a function of the perecent moisture content, w (the ratio of the mass of water to the mass of ovendry wood), can be described by

$$R = \frac{A}{1 + e^{C - Bw}} \quad (1)$$

Where A, B and C are fitting parameters. The parameters B (0.835) and C (19.8) are taken from a curve fit of the published data of Short and Dennis (Short & Dennis 1997). The parameter A, which is physically the asymptotic corrosion limit, is taken as 52.3 μm yr^{-1} from recent electrochemical measurements of hot-dip galvanized steel in an extract of ACQ treated southern pine (Zelinka et al. 2008). A graph of the corrosion rate as a function of moisture content is shown in Figure 2. It is noteworthy that no temperature dependence is included in the model at this stage; a further discussion of this is included in the "Future Work" section..

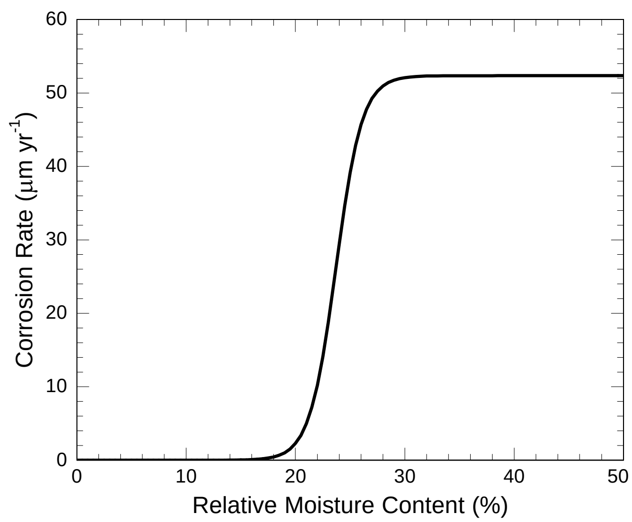

Figure 2: Corrosion model used in this study derived from (Zelinka et al. 2008) *and* (Short & Dennis 1997).

[1] For more information on the relationship between polarization resistance and the corrosion rate, see classic work by Mansfeld (1973).

Heat and Moisture Transport Modeling

The heat and moisture transport is calculated with a finite element code which uses capillary pressure[2] as the driving potential for moisture transport and temperature for heat transport (Janssen et al. 2007). The model can handle the full range of moisture content of wood from dry to capillary saturation as it includes liquid transport. The non-linearity as well as the temperature and moisture content dependence of the material properties are implemented.

In terms of boundary conditions, full atmospheric boundary conditions including air temperature and relative humidity, rain, wind, short-wave and long-wave solar radiation are applied on the top surface. On the "side" and "bottom" surfaces (Figure 1), only the air temperature and relative humidity are accounted for; the heat and mass transfer coefficients were taken as constant on these surfaces. The climatic data file comes from the hourly weather data collected at the Dane County Regional Airport (Madison, WI) from calendar year 2009. The solar radiation values were calculated from the model of Kittler (1981). The simulation is run from October 1 until September 30 to avoid having the simulation start in the middle of a season. The total precipitation is 1.106 m with a maximum rainfall intensity of 51mm hr^{-1}.

The temperature and moisture content of the wood at each node are written to an output file at one hour intervals.

Material Properties

The accuracy to which the hygrothermal model can predict the wood moisture content, and thus the corrosion rate, is dependent on appropriately determined material properties. The model requires a full moisture retention curve over both the hygroscopic (sorption isotherm) and overhygroscopic regimes. Furthermore, the vapor and liquid water conductivities are needed.

There are few published measurements on the hygrothermal properties of treated southern pine. Sorption isotherms of preservative-treated and untreated southern pine have recently been published (Zelinka & Glass 2010) and there were only small differences between the isotherms of ACQ, CCA, and untreated southern pine. Two other papers have collected sorption isotherms of treated southern pine (Cao & Kamdem 2004; Shupe et al. 2001). However, none of the papers have examined the vapor permeability of treated wood or characterized its overhygroscopic regime.

In the present work, the material properties have come from work on untreated Scots pine (*Pinus sylvestris*) (Zillig et al. 2006). While it is likely that there are differences in the hygrothermal

---

[2] Capillary pressure (p_c), the difference between the liquid and vapor pressure, can be related to relative humidity (φ)through the Kelvin equation: $\varphi = \exp\left(-p_c/\rho_l R_v T\right)$ where ρ_l is the density of liquid water, R_v is the gas constant and T is the absolute temperature.

properties of Scots pine and the southern pines, the data were chosen because of the quality and completeness of the data and because the data are from the same genus as the species group of interest. The moisture retention curve is shown in Figure 3. Volumetric moisture content, in kg m^{-3}, was based upon dry volume and this analysis thus ignores swelling and shrinkage. The liquid, vapor, and total permeabilities were taken from measurements in the tangential direction, and utilized the diffusivity approach presented by Carmeliet et al. (2007). The permeability as a function of capillary pressure is given in Figure 4. Heat capacities and thermal conductivity values for loblolly pine (*Pinus taeda*) were taken from the *Wood Handbook* (Glass & Zelinka 2010). The effect of temperature and wood moisture content on the heat capacity and thermal conductivity was ignored in this analysis.

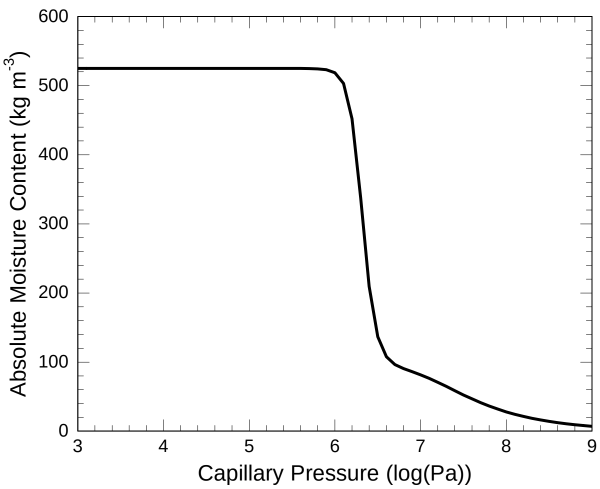

Figure 3: Moisture retention curve used in the hygrothermal model based on measurements from (Zillig et al. 2006).

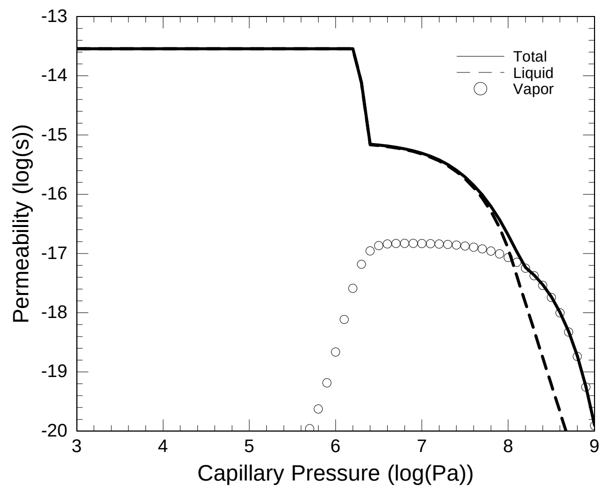

Figure 4: Liquid, vapor, and total permeabilities used in the hygrothermal model based on measurements from (Zillig et al. 2006) *and the approach of* (Carmeliet et al. 2007)*. The transition between* 10^6 *and* 10^7 *Pa corresponds to roughly 95% RH.*

Coupling Models

Modeling the corrosion of fasteners in treated wood involves two steps; first, calculating the wood moisture content, and secondly, calculating the metal corrosion rate, which is dependent on this moisture content. We calculate the corrosion rate at each output time step (every hour) at each node along the wood-metal interface from Eq (1) and the wood moisture content. We assume the corrosion rate to be constant over the entire hour and independent of temperature. The total amount of corrosion is found by summing the hourly amounts.

Results and Discussion

In this section, we present and discuss the results of a 1 year simulation. We then present the results of a sensitivity study varying some parameters and analyzing the effect on the corrosion profile.

Results of a 1 Year Simulation

The cumulative corrosion along the length of the fastener after a one year simulation is shown in Figure 5. The corrosion was non-uniform along the fastener depth resulting from the non-uniform moisture contents. The maximum corrosion occurred approximately 2.5 mm below the surface which can be explained by the competing wetting and drying processes. After a rain event, the surface of the wood has the highest moisture content but is also the first to dry following the rain event because of wind and solar radiation. Practically no corrosion occurred at fastener depths greater than 15 mm; the calculated corrosion rates in this region did not change with time, which suggests that the wood moisture content in this region only experienced small changes within the first year and remained below the corrosion threshold.

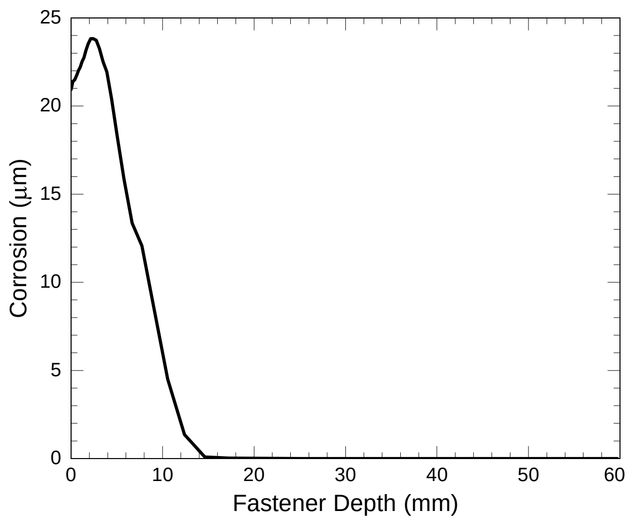

Figure 5: Corrosion rate as a function of depth for the "baseline" case described in the Results and Discussion section.

Sensitivity Study

An analysis was conducted to examine the effects of several of the parameters in the model on the corrosion rate. Parameters were examined by running a 1-year simulation with the parameter in a "low" state, in which the parameter was halved, or a "high" state where the parameter was doubled (Table 1). The parameters tested were: starting moisture content, heat capacity, thermal conductivity, solar radiation, and rainfall. The thermal properties were examined in particular since they were assumed to be independent of temperature and moisture content in all simulations. The solar radiation and rainfall were varied by multiplying the hourly values by 0.5 or 2, which changed both the intensity and total annual amount. An additional examination of rainfall was made by changing the climate file so that each rain event was half of the intensity of the baseline but had twice the duration. This simulation had the same annual rainfall as the baseline simulation but two times the number of hours during which precipitation occurred. The mesh sensitivity was examined by running a mesh with roughly half the number of elements (903 instead of 1965). A description of the parameters, numerical values used in the simulations, and the resulting changes in corrosion are compiled in Table 1.

Figure 6a gives the corrosion depth profile for several of the simulations from the sensitivity study. The maximum depth shown has been reduced to 10 mm so that y-axis could be scaled to highlight differences. Data from the simulations on heat capacity, mesh, and starting moisture content are not shown as they are too similar to the baseline case to be differentiated clearly at this scale. The differences due to changing thermal conductivity and solar radiation highlight the importance of solar drying on the top surface of the beam.

Table 1: Parameters varied and resulting changes on the maximum corrosion rate in the sensitivity analyses for one year simulations.

Parameter	Baseline values	Case	Maximum Corrosion Depth (μm)	Absolute Difference (μm)	Percent Difference
Baseline			23.80	-	-
Mesh	1965 elements	Coarse (903)	23.73	-0.07	0.3%
Heat capacity	1240 J kg^{-1} K^{-1}	Low (620)	23.92	0.12	0.5%
		High (2480)	23.67	-0.13	0.6%
Starting MC	12%	Low (3.6%)	23.59	-0.21	0.9%
		High (20%)	24.18	0.38	2%
Total annual rainfall	1.106 m	Low (0.55)	22.27	-1.54	6%
		High (2.21)	24.71	0.90	4%
Thermal conductivity	0.11 W m^{-1} K^{-1}	Low (0.055)	25.90	2.10	9%
		High (0.22)	22.11	-1.69	7%
Total annual solar radiation	7.41 GJ m^{-2}	Low (3.70)	28.61	4.81	20%
		High (14.8)	19.09	-4.71	20%
Number of hours with rainfall	696 hours	High (1392)	31.57	7.77	33%

At first glance, it may seem surprising that doubling the total annual rainfall has a small apparent affect on the total amount of corrosion. This is likely the result of the manner in which the total amount of rainfall was doubled—by doubling the intensity of all rain events. Although the total amount of rainfall was doubled by this method, the number of hours with rain remained the same. The total amount of water absorbed by wood on surfaces without end grain during a rain event is apparently limited more by the absorption rate than the total amount of water, and therefore the corrosion rate is relatively unaffected by the increased rainfall intensity. This is confirmed by the second simulation that varied the number of hours of rainfall but kept the total annual precipitation constant, as shown in Figure 6b. It is clear that the corrosion of fasteners is dependent not only on the total amount of annual rainfall but also the frequency and duration of the rain events.

The variations in parameters utilized in the sensitivity analysis represent extreme values. Even with these unphysically high or low values, the corrosion rate did not experience large fluctuations. For example, the maximum amount of corrosion only changed by 20% with a 200% change in solar radiation (Table 1).

The baseline value of 0.11 W m^{-1} K^{-1} corresponds to dry wood (0% MC) at room temperature. At a value of 25% MC the thermal conductivity would increase to about 0.17 W m^{-1} K^{-1} (a 55% increase). Given that a 100% increase in the thermal conductivity caused a 7% change in the maximum corrosion rate, it appears that the results could be improved slightly by implementing the dependence of moisture on the thermal conductivity

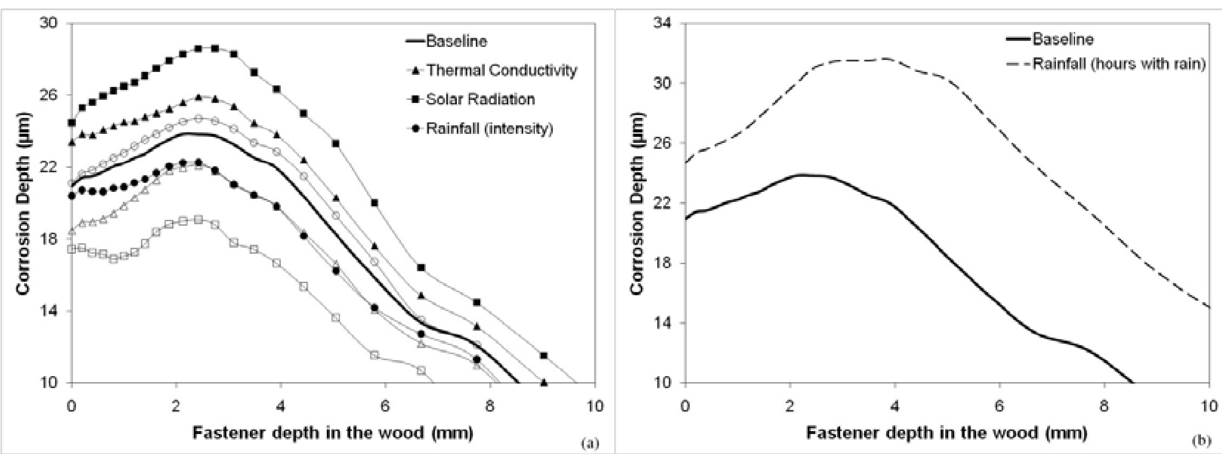

Figure 6(a): Selected results of the sensitivity study. The filled shapes represent scaling the parameter by a factor of 0.5 and the open shapes by a factor of 2. 6(b): Comparison of the baseline to the simulation in which the number of hours of rainfall was doubled (note the difference in scale).

Future Work

While the preliminary model successfully identified key trends, several improvements can be made to the model. Future work will further develop the current model to include the following three issues: temperature dependence of the corrosion rate, better determined treated wood material properties, and inclusion of heat transport in the nail.

The current model assumes the temperature has no effect on the corrosion rate. This is an over-simplification. The simplest model for atmospheric corrosion, the ISO-9223 "Time of Wetness" model assumes that atmospheric corrosion occurs when the relative humidity of the air is greater than 80% and the temperature is greater than 0°C (anon. 1992). A first improvement to the coupled model could be made by enforcing a no corrosion condition when the temperature is below freezing. While more advanced kinetic models exist for the effect of changes in temperature on atmospheric corrosion rates above freezing, there are not enough data yet on corrosion of metals in wood at different temperatures to provide a reliable enough model.

It is likely that treated southern pine has different material properties than the properties of untreated Scots pine used in this model. There are differences in wood anatomy between these two species which may affect the overhygroscopic moisture retention curve as this is sensitive to the pore size distribution of the material (Roels et al. 2001). Furthermore, although it has been shown that the treatment chemicals themselves are not hygroscopic (Zelinka & Glass 2010), the treatment process subjects the wood to large pressure differentials. It is possible that during treatment, this pressure gradient creates new pores, mainly by damaging bordered pits, changes the dimensions of existing pores, or changes the accessibility of existing pores. A full investigation of the hygrothermal properties of treated southern pine is planned for use in future modeling.

Another improvement to be made to the model is the simulation of the heat transfer through the nail. In the current simulation, the nail is represented by a "no-flow" boundary condition. While it is likely that this assumption is valid for moisture transport, it is clearly not physical for heat transfer as the high thermal conductivity of the nail should act as a thermal bridge and the resulting heat transported by the nail will certainly affect the moisture distribution in the wood close to the contact area.

Once the model is developed, it can be used to evaluate different construction and maintenance practices such as decking materials and water repellent treatments.

Conclusions

This paper presents a preliminary modeling investigation coupling a heat and mass transport model and a corrosion model to assess the corrosion of fasteners embedded in wood. Using this model, the corrosion profile after one year of exposure was simulated for a steel nail embedded in ACQ wood.

The maximum amount of corrosion occurred between 2 and 4 mm below the wood surface. Practically no corrosion occurred at depths greater than 15 mm below the surface. This corrosion profile was calculated from a corrosion rate that depends only on moisture content, and therefore the differences in corrosion with depth result only from the wood moisture content profile.

An initial sensitivity study showed that the amount of corrosion was most sensitive to the number of hours of rain. The amount of corrosion was not sensitive to the starting moisture content (below 20%) or the heat capacity of the wood.

Future work will focus on including the temperature dependence of the corrosion rate, including heat transfer through the fastener, and using material properties measured in treated southern pine.

Acknowledgement

We would like to acknowledge the contributions and support of Jan Carmeliet, Peter Moonen, and Hannelore Derluyn of Empa (Dübendorf, Switzerland) as well as C.R. Boardman of the US Forest Products Laboratory.

References

anon, 2007. *AWPA U1-06: Use category system*, Granbury, TX: American Wood Preservers' Association.

anon., 1992. *ISO 9223 Corrosion of metals and alloys- corrosivity of atmospheres-classification*, Geneva, Switzerland: International Organization for Standardization.

anon., 2008. *Preservative treated wood*, Simpson Strong-Tie Technical Bulletin. Available at: http://www.strongtie.com/literature/tech-bulletins.html.

Baker, A.J., 1987. Corrosion of metals in preservative-treated wood. In M. Hamel, ed. Memphis, TN: Forest Products Research Society, pp. 99-101.

Burkholder, M., 2004. CCA, NFBA, and the post-frame building industry. *Frame Building News*, 16(5), 6-12.

Cao, J. & Kamdem, D.P., 2004. Moisture adsorption characteristics of copper-ethanolamine (Cu-EA) treated Southern yellow pine (Pinus spp.). *Holzforschung*, 58(1), 32-38.

Carmeliet, J., Janssen, H. & Derluyn, H., 2007. An improved moisture diffusivity model for porous building materials. In *Proceedings of the 12th Symposium for Building Physics*. Proceedings of the 12th Symposium for Building Physics. Desden, Germany.

Freeman, M. & McIntyre, C., 2008. A comprehensive review of copper-based wood preservatives with a focus on new micronized or dispersed copper systems. *Forest Products Journal*, 58(11), 6-27.

Glass, S.V. & TenWolde, A., 2007. *Review of In-Service moisture and temperature conditions in wood-frame buildings. Gen. Tech. Rp. FPL-GTR-174*, U.S. Department of Agriculture, Forest Service, Forest Products Laboratory.

Glass, S. & Zelinka, S.L., 2010. Moisture Relations and Physical Properties of Wood. In R. Ross,, ed. *Wood Handbook. Centennial Edition. FPL-GTR-190*. U.S. Department of Agriculture, Forest Service, Forest Products Laboratory.

Janssen, H., Blocken, B. & Carmeliet, J., 2007. Conservative modelling of the moisture and heat transfer in building components under atmospheric excitation. *International Journal of Heat and Mass Transfer*, 50(5-6), 1128-1140.

Kear, G., Wu, H. & Jones, M.S., 2009. Weight loss studies of fastener materials corrosion in contact with timbers treated with copper azole and alkaline copper quaternary compounds. *Corrosion Science*, 51(2), 252-262.

Kittler, R., 1981. A universal calculation method for simple predetermination of natural radiation on building surfaces and solar collectors. *Building and Environment*, 16(3), 177-182.

Lebow, S. & Lebow, P., 2007. The role of moisture in above-ground leaching. In *Proceedings of the 38th annual meeting of the International Group on Wood Preservation*. Jackson Hole, Wyoming, USA: IRG Secretariat.

Lebow, S., 2004. *Alternatives to Chromated Copper Arsenate for Residential Construction. Res. Pap. FPL-RP-618*, U.S.D.A. Forest Service, Forest Products Laboratory, Madison, WI.

Mansfeld, F., 1973. Tafel slopes and corrosion rates from polarization resistance measurements. *Corrosion*, 29(10), 397-402.

Roels, S. et al., 2001. Characterisation of pore structure by combining mercury porosimetry and micrography. *Materials and Structures*, 34(2), 76-82.

Short, N.R. & Dennis, J.K., 1997. Corrosion resistance of zinc-alloy coated steel in construction industry environments. *Transactions of the Institute of Metal Finishing*, 75(2), 47-52.

Shupe, T.F. et al., 2001. Inadequate redrying linked to dimensional instability of CCA-treated southern pine lumber. *Forest Products Journal*, 51(5), 59-62.

West, A., 2006. Deck inspections: A matter of life and death. *Wood Design Focus*, 16(2), 22-24.

Zelinka, S.L. & Glass, S.V., 2010. Water vapor sorption isotherms for southern pine treated with several waterborne preservatives. *ASTM Journal of Testing and Evaluation*, 38(4), tbd.

Zelinka, S.L. & Rammer, D.R., 2009. Corrosion rates of fasteners in treated wood exposed to 100% relative humidity. *ASCE Journal of Materials in Civil Engineering*, 21(12), 758-763.

Zelinka, S.L., Rammer, D.R. & Stone, D.S., 2008. Electrochemical corrosion testing of fasteners in wood extract. *Corrosion Science*, 50(5), 1251-1257.

Zillig, W. et al., 2006. Liquid water transport in wood: Towards a mesoscopic approach. In Ge, Rao, & Desmarais, eds. *Research in Building Physics and Building Engineering*. London: Taylor and Francis Group.